Amine-Functionalized Quantum Dots as Universal Fluorescent Nanoprobe for One-Step Loop-Mediated Isothermal Amplification Assay with Single-Copy Sensitivity

Shiyao Wang,[a,§] Ailin Qin,[a,§] Li Yin Chau,[a] Eunice W. T. Fok,[b] Mei Yue Choy,[b] Christopher J. Brackman,[b] Gilman K. H. Siu,[c] Chien-Ling Huang,[c] Shea Ping Yip,[c,] and Thomas M. H. Lee[a,]**

[a]Department of Biomedical Engineering, The Hong Kong Polytechnic University, Hung Hom, Kowloon, Hong Kong 000000, China

[b]Agriculture, Fisheries and Conservation Department, Government of the Hong Kong Special Administrative Region, Hong Kong 000000, China

[c]Department of Health Technology and Informatics, The Hong Kong Polytechnic University, Hung Hom, Kowloon, Hong Kong 000000, China

KEYWORDS: quantum dots, loop-mediated isothermal amplification, nucleic acid testing, lambda DNA, SARS-CoV-2 RNA, avian influenza virus RNA

ABSTRACT: Loop-mediated isothermal amplification (LAMP) has received considerable attention for decentralized (point-of-care and on-site) nucleic acid testing in view of its simple temperature control (60–65 °C) and short assay time (15–60 min). There remains challenge in its wide adoption and acceptance due to the limitations of the existing amplification result reporter probes, e.g., photobleaching of organic fluorophore and reduced sensitivity of pH-sensitive colorimetric dye. Herein, we demonstrate CdSeS/ZnS quantum dots (semiconductor fluorescent nanocrystals with superior photostability than organic fluorophore) with surface modification of cysteamine (amine-QDs) as a new reporter probe for LAMP that enabled single-copy sensitivity (limit of detection of 83 zM; 20 μL reaction volume). For a negative LAMP sample (absence of target sequence), positively charged amine-QDs remained dispersed due to interparticle electrostatic repulsion. While for a positive LAMP sample (presence of target sequence), amine-QDs became precipitated. The characterization data showed that amine-QDs were embedded in magnesium pyrophosphate crystals (generated during positive LAMP), thus leading to their coprecipitation. This amine-QD-based one-step LAMP assay advances the field of QD-based nucleic acid amplification assays in two aspects: (1) compatibility—one-step amplification and detection (versus separation of amplification and detection steps); and (2) universality—the same amine-QDs for different target sequences (versus different oligonucleotide-modified QDs for different target sequences).

1. INTRODUCTION

The coronavirus disease 2019 (COVID-19) pandemic has spurred the development of point-of-care and on-site nucleic acid testing. Compared with thermocycling amplification such as

polymerase chain reaction (PCR; current nucleic acid amplification test gold standard),[1] isothermal amplification is better suited for decentralized nucleic acid testing in view of simpler temperature control instrumentation (thus not only lower equipment cost but also shorter assay time).[2] Over the past 30 years, various isothermal amplification techniques have been developed, such as nucleic acid sequence-based amplification (NASBA),[3] strand displacement amplification (SDA),[4] rolling circle amplification (RCA),[5] loop-mediated isothermal amplification (LAMP),[6] exponential amplification reaction (EXPAR),[7] helicase-dependent amplification (HDA),[8] and recombinase polymerase amplification (RPA).[9] Among them, LAMP is particularly attractive due to room temperature storage of lyophilized reagents[10,11] as well as direct amplification of unpurified specimens.[12–16] LAMP has two salient features—utilizing DNA polymerase with strand displacement activity (such as *Bst* DNA polymerase of optimal operating temperature at 60–65 °C) and involving four to six specially designed primers—that enable a specific sequence to be amplified to 10^9 copies in 15–60 minutes.[6,17,18] There are three common LAMP result readout methods, including fluorimetry (small organic DNA intercalating dyes[19,20] and small organic fluorophore-labeled oligonucleotide probes[15,16,21]), turbidimetry (magnesium pyrophosphate ($Mg_2P_2O_7$) crystals formation[22,23]), and colorimetry (divalent cation-sensitive[24] and pH-sensitive[25] dyes). But new readout method is still highly desired because of the limitations of the existing methods, including photobleaching of small organic intercalating dyes and fluorophore-labeled oligonucleotide probes, inapplicability for turbid specimens, as well as interference by specimen's divalent cations and pH.

Quantum dot (QD; fluorescent inorganic semiconductor nanocrystal; e.g., CdSe/ZnS core/shell QD) is potentially a promising new isothermal amplification reporter for decentralized testing thanks to its superior photostability.[26] Nevertheless, to date, only very few attempts have been

made to develop QD-based isothermal amplification assay platforms. Bakalova, Ohba, and co-workers developed an assay platform with messenger RNA target sequence amplification by NASBA in the presence of Cy5-labeled nucleotides, followed by hybridization and detection (fluorescence resonance energy transfer, FRET) between Cy5-labeled amplicons and QD–oligonucleotide probe conjugates.[27] Zhang and co-workers developed an assay platform with microRNA target sequence amplification by hyperbranched RCA, followed by sandwich hybridization among amplicons, Cy3-labeled oligonucleotide probes, and biotin-labeled oligonucleotide probes, then binding to QD–streptavidin conjugates, and finally detection (FRET).[28] It should be pointed out that these two assay platforms involved postamplification open-tube addition of the detection probes (including the QD-based probes) attributed to incompatibility issue, which not only increased the risk of carryover contamination but also increased the assay time. On the other hand, a few closed-tube/one-step QD-based PCR platforms have been reported.[29–31] Wang, Xu, and co-workers[29] and Pang, Li, and co-workers[30] demonstrated that oligonucleotides/primers bound to QDs were successfully extended in the presence of specific complementary target sequences during PCR. Despite the excellent detection performance of QD–oligonucleotide probe conjugates, their preparation is costly (oligonucleotide with attachment functional group; typically prepared via ligand exchange with thiol-modified oligonucleotide). Besides, different QD–oligonucleotide probe conjugates are needed for different target sequences (poor universality). The only exception was the work reported by Cui and co-workers that mercaptoacetic acid-modified CdTe QDs could achieve real-time monitoring of PCR, but the underlying mechanism was not clear.[31]

In this work, we report a first-of-its-kind universal QD probe (same probe for different target sequences) for closed-tube monitoring of LAMP assay. Specifically, cysteamine-modified

CdSeS/ZnS QDs (amine-QDs) enable a clear differentiation between negative (absence of target sequence) and positive (presence of target sequence) LAMP samples, as illustrated in Scheme 1. For a negative LAMP sample, amine-QDs remain dispersed as a result of interparticle electrostatic repulsion (amine-QDs are positively charged). For a positive LAMP sample, $Mg_2P_2O_7$ crystals are produced along with target sequence amplification.[22,23] Amine-QDs are embedded in $Mg_2P_2O_7$ crystals (amine–pyrophosphate interaction) and thus coprecipitation occurs. Besides excellent universality, worry-free carryover contamination control, simple constant temperature control, and short assay time, this new assay platform has superior sensitivity. With lambda DNA and SARS-CoV-2 RNA as model templates, single-copy detection was demonstrated. Its applicability to real-sample testing was exemplified with avian influenza virus RNA detection from live chicken swab.

Scheme 1. Schematic illustration of the one-step loop-mediated isothermal amplification (LAMP) assay with cysteamine-modified CdSeS/ZnS quantum dots (amine-QDs). The drawing is not to scale (amine-QD: 6 nm; magnesium pyrophosphate ($Mg_2P_2O_7$) crystal: ~0.5–0.8 μm).

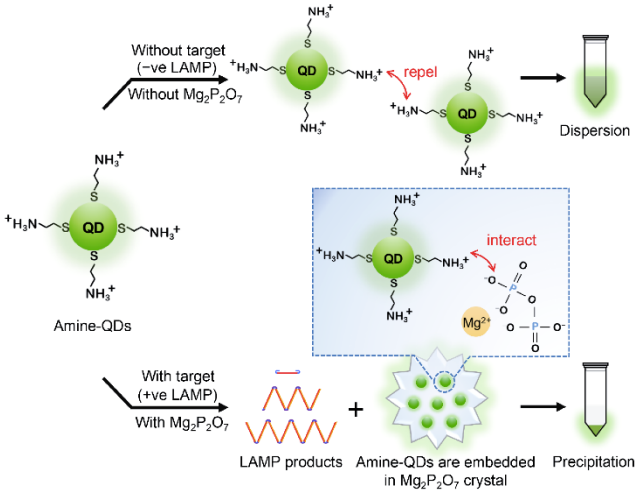

2. EXPERIMENTAL SECTION

2.1. Materials and Instruments. Oleic acid-capped CdSeS/ZnS QDs (diameter of 6 nm; emission peak at 540 nm, green color; dispersed in toluene), chloroform, methanol, acetone, hexane, cysteamine hydrochloride, tris(hydroxymethyl)aminomethane (Tris), hydrochloric acid (HCl), potassium pyrophosphate ($K_4P_2O_7$), betaine solution (5 M), and agarose powder were purchased from Merck Sigma-Aldrich. UltraPure DNase/RNase-free distilled water (UltraPure water), 10,000× SYBR Green I nucleic acid gel stain, 10× Tris–borate–ethylenediaminetetraacetic acid (TBE) buffer, and 10× Orange DNA loading dye were purchased from Thermo Fisher Scientific. Amicon Ultra-0.5 centrifugal filter unit (10 kDa cutoff) was purchased from Merck Millipore. Isothermal amplification buffer (10×), deoxynucleotide solution mix (deoxynucleoside triphosphates, dNTPs; 10 mM each), *Bst* 2.0 DNA polymerase, lambda DNA, low molecular weight DNA ladder, pBR322 DNA, magnesium sulfate solution ($MgSO_4$; 100 mM), WarmStart reverse transcriptase, and AMV reverse transcriptase were purchased from New England Biolabs. All oligonucleotides were purchased from Integrated DNA Technologies. Black polystyrene 384-well microplate was purchased from Greiner. QuantiFast Pathogen PCR +IC kit and QuantiFast Pathogen RT-PCR +IC kit were purchased from QIAGEN. AmpliRun DNA/RNA amplification controls were purchased from Vircell (SARS-CoV-2 RNA, *Bordetella pertussis* DNA, *Haemophilus influenzae* DNA, influenza A H1 RNA, Middle East respiratory syndrome coronavirus RNA, *Mycobacterium tuberculosis* DNA, *Mycoplasma pneumoniae* DNA, parainfluenza 1 RNA, parainfluenza 4A RNA, rhinovirus RNA, SARS (2003) coronavirus RNA, and *Streptococcus pneumoniae* DNA; all provided with known batch concentrations). All solutions were prepared with UltraPure water.

Centrifugation was carried out using a Centrifuge 5415D (Eppendorf). Sonication was carried out using a WiseClean WUC-A01H ultrasonic cleaner (DAIHAN Scientific). Visible absorption spectrum was acquired using an Ultrospec 2100 pro UV/visible spectrophotometer (GE Healthcare). Zeta potential was acquired using a Zetasizer Nano ZS (Malvern; 633 nm He–Ne laser). Isothermal incubation was carried out using a GeneAmp PCR System 9700 (Applied Biosystems). Fluorescence excitation was carried out using an EN-280L/FE 365 nm ultraviolet lamp (Spectroline). Transmission electron microscopy (TEM) analysis was conducted by a JEM-2100F field emission electron microscope (JEOL; integrated with energy-dispersive X-ray spectroscopy (EDS)). Confocal microscopy analysis was conducted by a TCS SPE confocal microscope (Leica). Gel electrophoresis analysis was conducted by a Gel Doc XR+ System (Bio-Rad). Fluorescence measurement was performed using a Synergy HTX multi-mode reader (BioTek). Real-time polymerase chain reaction (qPCR) and real-time reverse transcription–polymerase chain reaction (RT-qPCR or qRT-PCR) were carried out using a LightCycler 480 Instrument II (Roche). Purification of oropharyngeal/cloacal swab samples collected from live chickens was carried out using a MagNA Pure 96 Instrument (Roche).

2.2. Synthesis and Characterization of Amine-QDs. The preparation of amine-QDs was based on a reported ligand exchange method with modifications.[32] Briefly, 200 μL of 1 mg/mL oleic acid-capped CdSeS/ZnS QDs was mixed with 200 μL of chloroform, 200 μL of methanol, and then 2 mL of acetone, followed by centrifugation at 13.2 krpm for 20 min. After the removal of the supernatant, 200 μL of hexane was added to resuspend the precipitate. Next, 2 mL of acetone was added, followed by centrifugation at 13.2 krpm for 20 min. The precipitate (supernatant removed) was dried under vacuum at room temperature for 1 h. The dried precipitate was resuspended in 300 μL of chloroform. Subsequently, 1 mL of 50 mg/mL cysteamine hydrochloride

was added. The resultant two immiscible layers were sonicated for 10 min and left to stand for 20 s (the bottom layer became colorless). The top layer containing amine-QDs was collected and the excess cysteamine was removed by centrifugal ultracentrifugation (12.3 krpm for 10 min; the concentrate was reconstituted to its original volume; repeated centrifugation, reconsititution, and centrifugation). The prepared amine-QDs were stored at 4 °C until use. It should be noted that the volume of the final purified concentrate was about one-tenth of the original, i.e., amine-QDs were concentrated by about ten times. The concentration of amine-QDs was estimated based on the extinction coefficient of oleic acid-capped CdSeS/ZnS QDs (210,000 $M^{-1}cm^{-1}$ at 517 nm; provided by the manufacturer) and the absorbance at 517 nm according to the Beer–Lambert law. Zeta potentials of amine-QDs at different pHs (5–9; with 20 mM Tris-HCl) were measured.

2.3. Mechanistic Study of Dispersion and Precipitation Behavior of Amine-QDs under Simulated LAMP Conditions. Simulated positive LAMP sample (20 μL) containing 1× isothermal amplification buffer (20 mM Tris-HCl, 10 mM $(NH_4)_2SO_4$, 50 mM KCl, 2 mM $MgSO_4$, and 0.1% Tween 20; pH 8.8) and 1.4 mM $K_4P_2O_7$, simulated negative LAMP sample with amine-QDs (20 μL) containing 1× isothermal amplification buffer and 60 nM amine-QDs, as well as simulated positive LAMP sample with amine-QDs (20 μL) containing 1× isothermal amplification buffer, 1.4 mM $K_4P_2O_7$, and 60 nM amine-QDs were prepared. These three samples were incubated at 65 °C for 1 h and visualized under ultraviolet excitation (365 nm). For TEM analysis, these three samples were washed three times by centrifugation (5.8 krpm for 15 min) and redispersion (20 μL of UltraPure water). The samples (2 μL) were applied onto carbon-coated copper grids and dried under ambient conditions. The simulated positive LAMP sample with amine-QDs was also analyzed by EDS.

Zeta potentials of $Mg_2P_2O_7$ crystals (200 µL of 2 mM $MgSO_4$ and 1.4 mM $K_4P_2O_7$; diluted with 600 µL of 26.7 mM Tris-HCl, pH 8.8), amine-QDs (200 µL of 60 nM amine-QDs; diluted with 600 µL of 26.7 mM Tris-HCl, pH 8.8), and amine-QDs with $P_2O_7^{4-}$ (200 µL of 60 nM amine-QDs and 1.4 mM $K_4P_2O_7$; diluted with 600 µL of 26.7 mM Tris-HCl, pH 8.8) were measured in triplicate.

A preformed $Mg_2P_2O_7$ with amine-QDs sample was prepared similar to the simulated positive LAMP sample with amine-QDs, except that isothermal amplification buffer and $K_4P_2O_7$ (17 µL) were first incubated at 65 °C for 30 min (amine-QDs (3 µL of 400 nM stock) were then added and further incubated at 65 °C for 1 h). This sample and the simulated positive LAMP sample with amine-QDs were visualized under ultraviolet excitation (365 nm). For confocal microscopy analysis, the samples (20 µL) were redispersed by pipetting, added onto confocal dishes, and dried under ambient conditions.

Another set of simulated experiments was carried out, including amine-QDs in isothermal amplification buffer (identical to the simulated negative LAMP sample with amine-QDs), amine-QDs in isothermal amplification buffer with $K_4P_2O_7$ (identical to the simulated positive LAMP sample with amine-QDs), and amine-QDs in isothermal amplification buffer with dNTPs (1.4 mM total; 0.35 mM each). These three samples were incubated at 65 °C for 1 h and visualized under ultraviolet excitation (365 nm).

2.4. LAMP with Lambda DNA. Six LAMP primers were utilized for amplifying lambda DNA, including lambda-FIP (5′-CAGCCAGCCGCAGCACGTTCGCTCATAGGAGATATGGTAGAGCCGC-3′), lambda-BIP (5′-GAGAGAATTTGTACCACCTCCCACCGGGCACATAGCAGTCCTAGGGACAGT-3′), lambda-F3 (5′-GGCTTGGCTCTGCTAACACGTT-3′), lambda-B3 (5′-

GGACGTTTGTAATGTCCGCTCC-3′), lambda-LF (5′-CTGCATACGACGTGTCT-3′), and lambda-LB (5′-ACCATCTATGACTGTACGCC-3′).[17] LAMP samples (20 μL) comprised 1× isothermal amplification buffer (20 mM Tris-HCl, 10 mM $(NH_4)_2SO_4$, 50 mM KCl, 2 mM $MgSO_4$, and 0.1% Tween 20; pH 8.8), lambda-FIP (0.8 μM), lambda-BIP (0.8 μM), lambda-F3 (0.2 μM), lambda-B3 (0.2 μM), lambda-LF (0.4 μM), lambda-LB (0.4 μM), amine-QDs (40 nM), betaine (1 M), *Bst* 2.0 DNA polymerase (0.32 units/μL), dNTPs (1.4 mM; 0.35 mM each), and lambda DNA (negative: 0 copies; positive: 10^5 copies). Samples without amine-QDs were also included. After incubation at 65 °C for 1 h, the samples were visualized under ultraviolet excitation (365 nm). Besides, the samples were analyzed by TEM (identical preparation procedures as the simulated LAMP samples Section 2.3). Agarose gel electrophoresis analysis of the samples was also conducted. The samples (8 μL), together with a DNA ladder, were mixed with SYBR Green I nucleic acid gel stain (1 μL of 100×; the 10,000× stock was diluted with 0.5× TBE buffer: 45 mM Tris, 45 mM boric acid, and 1 mM ethylenediaminetetraacetic acid; pH 8.0) and incubated in darkness at room temperature for 15 min. Next, Orange DNA loading dye (2 μL) was added, followed by loading into an agarose gel (2 wt % in 0.5× TBE buffer) and electrophoresis at 100 V for 50 min. The gel was then visualized under UV transillumination. Another positive sample without amine-QDs was prepared. After incubation at 65 °C for 1 h, the sample was centrifuged (2 krpm for 1 min). The supernatant (17 μL) was directly mixed with amine-QDs (3 μL of 400 nM). The precipitate was washed three times by centrifugation (2 krpm for 30 s) and redispersion (15 μL of UltraPure water), then mixed with amine-QDs (3 μL of 400 nM) and 10× isothermal buffer (2 μL). Both samples were further incubated at 65 °C for 1 h and visualized under ultraviolet excitation (365 nm).

For specificity test, four different template combinations of lambda DNA (specific template) and pBR322 DNA (nonspecific template) were included, i.e., no template, lambda DNA only, pBR322 DNA only, and lambda DNA plus pBR322 DNA. For sensitivity test, different copy numbers of lambda DNA (0, 10, 10^2, 10^3, 10^4, and 10^5) were included. For both tests, after incubation at 65 °C for 1 h, the samples were visualized under ultraviolet excitation (365 nm). Agarose gel electrophoresis analysis of the samples was also conducted. Additional samples containing 10^3 and 10^5 copies were included. At different time points of the LAMP reaction (0, 10, 20, 30, 40, 50, and 60 min), one sample for each copy number was taken out and centrifuged (2 krpm for 30 s). The fluorescence intensities of the supernatants were measured (15 μL; black polystyrene microplate; excitation at 360 nm and detection at 530 nm). Another sensitivity test (copy numbers: 0, 1, 10, 10^2, 10^3, 10^4, and 10^5; triplicate for each) was performed with higher concentrations of Mg^{2+} (8 mM versus 2 mM), primers (lambda-FIP and lambda-BIP, 1.6 μM each versus 0.8 μM each), and dNTPs (5.6 mM total/1.4 mM each versus 1.4 mM total/0.35 mM each). The samples were incubated at 65 °C for 40 min. For qPCR assays, samples (20 μL) comprised 1× QuantiFast Pathogen Master Mix, 1× Internal Control Assay, 1× Internal Control DNA, lambda-F (5′-TAAAG AGTCGAATGATGTTGGC-3′; 0.4 μM), lambda-R (5′-GGTCGCTAATACGCTAAA AGAT-3′; 0.4 μM), lambda-P (5′-FAM-AAATCACATCGTCACCCATT-BHQ1-3′; 0.2 μM), and lambda DNA (copy numbers: 0, 1, 10, 10^2, 10^3, 10^4, and 10^5). The sequences of the primers and TaqMan probe were adopted from a published work.[33] Temperature profile involved initial denaturation at 95 °C for 5 min, followed by 45 cycles of denaturation at 95 °C for 15 s and annealing/extension at 60 °C for 30 s. All qPCR assays were performed in triplicate.

2.5. RT-LAMP with SARS-CoV-2 RNA. Six RT-LAMP primers were utilized for amplifying SARS-CoV-2 RNA N gene, including SARS-CoV-2-N-FIP (5′-TCTGGCCCAGTTCCTAGGTA

GTCCAGACGAATTCGTGGTGG-3′), SARS-CoV-2-N-BIP (5′-AGACGGCATCATATGGGT TGCACGGGTGCCAATGTGATCT-3′), SARS-CoV-2-N-F3 (5′-TGGCTACTACCGAAGAGC T-3′), SARS-CoV-2-N-B3 (5′-TGCAGCATTGTTAGCAGGAT-3′), SARS-CoV-2-N-LF (5′-GG ACTGAGATCTTTCATTTTACCGT-3′), and SARS-CoV-2-N-LB (5′-ACTGAGGGAGCCTTG AATACA-3′).[34] Six RT-LAMP primers were utilized for amplifying SARS-CoV-2 RNA E gene, including SARS-CoV-2-E-FIP (5′-ACCACGAAAGCAAGAAAAAGAAGTTCGTTTCGGAAG AGACAG-3′), SARS-CoV-2-E-BIP (5′-TTGCTAGTTACACTAGCCATCCTTAGGTTTTACA AGACTCACGT-3′), SARS-CoV-2-E-F3 (5′-TGAGTACGAACTTATGTACTC AT-3′), SARS-CoV-2-E-B3 (5′-TTCAGATTTTTAACACGAGAGT-3′), SARS-CoV-2-E-LF (5′-CGCTATTA ACTATTAACG-3′), and SARS-CoV-2-E-LB (5′-GCGCTTCGATTGTGTGCGT-3′).[34] RT-LAMP samples (20 μL) comprised 1× isothermal amplification buffer, SARS-CoV-2-N/E-FIP (1.6 μM), SARS-CoV-2-N/E-BIP (1.6 μM), SARS-CoV-2-N/E-F3 (0.2 μM), SARS-CoV-2-N/E-B3 (0.2 μM), SARS-CoV-2-N/E-LF (0.4 μM), SARS-CoV-2-N/E-LB (0.4 μM), amine-QDs (40 nM), betaine (0.2 M), *Bst* 2.0 DNA polymerase (0.32 units/μL), dNTPs (5.6 mM; 1.4 mM each), $MgSO_4$ (6 mM), WarmStart reverse transcriptase (0.25 units/μL), and SARS-CoV-2 RNA (0–100 copies; triplicate for each). After incubation at 65 °C for 40 min, the samples were visualized under ultraviolet excitation (365 nm). Agarose gel electrophoresis analysis of the samples was also conducted (same protocol as that for lambda DNA). Two RT-qPCR primers and one TaqMan probe were utilized for amplifying and detecting SARS-CoV-2 RNA N gene, including SARS-CoV-2-N-F (5′-CACATTGGCACCCGCAATC-3′), SARS-CoV-2-N-R: 5′-GAGGAACGAGAA GAGGCTTG-3′), and SARS-CoV-2-N-P (5′-FAM-ACTTCCTCAAGGAACAACATTGCCA-BHQ1-3′).[35] Two RT-qPCR primers and one TaqMan probe were utilized for amplifying and detecting SARS-CoV-2 RNA E gene, including SARS-CoV-2-E-F (5′-ACAGGTACGTTAATAG

TTAATAGCGT-3′), SARS-CoV-2-E-R (5′-ATATTGCAGCAGTACGCACACA-3′), and SARS-CoV-2-E-P (5′-FAM-ACACTAGCCATCCTTACTGCGCTTCG-ZEN/IBFQ-3′).[35] For RT-qPCR assays, samples (20 μL) comprised 1× QuantiFast Pathogen Master Mix, 1× QuantiFast Pathogen RT Mix, 1× Internal Control Assay, 1× Internal Control RNA, SARS-CoV-2-N/E-F (N: 0.6 μM; E: 0.4 μM), SARS-CoV-2-N/E-R (N: 0.8 μM; E: 0.4 μM), SARS-CoV-2-N/E-P (N: 0.2 μM; E: 0.2 μM), and SARS-CoV-2 RNA (0–100 copies). Temperature profile involved RT at 50 °C for 20 min, initial denaturation at 95°C for 5 min, followed by 45 thermal cycles of denaturation at 95 °C for 15 s and annealing/extension at 60 °C for 30 s. All RT-qPCR assays were performed in triplicate. For specificity test with RT-LAMP, different templates were tested, including no template control, SARS-CoV-2 (specific template; 10^2 copies), and 11 nonspecific templates (10^3 copies; *Bordetella pertussis* DNA, *Haemophilus influenzae* DNA, influenza A H1 RNA, Middle East respiratory syndrome coronavirus RNA, *Mycobacterium tuberculosis* DNA, *Mycoplasma pneumoniae* DNA, parainfluenza 1 RNA, parainfluenza 4A RNA, rhinovirus RNA, SARS (2003) coronavirus RNA, and *Streptococcus pneumoniae* DNA). After incubation at 65 °C for 35 min, the samples were visualized under ultraviolet excitation.

2.6. RT-LAMP with Avian Influenza Virus RNA from Live Chicken Swab. Oropharyngeal/cloacal swab samples collected from live chickens were purified by MagNA Pure 96 Instrument to obtain RNA extracts. Different dilutions of the purified RNA extracts were prepared (10^{-3}–10^{-6}; 10^{-3} was equivalent to 10^3-fold dilution and 10^{-6} was equivalent to 10^6-fold dilution; UltraPure water). Six RT-LAMP primers were used for amplifying avian influenza virus RNA (H9 subtype), including AIV-H9-FIP (5′-GCCCCACATGAAAAGAATGTTCTTTGTTGACTCAAAAGAACAACGC-3′), AIV-H9-BIP (5′-AATCACCCACCCACTGATACTATCTTCTGTTGCCACACTTG-3′), AIV-H9-F3 (5′-CATTCTACAGAAGCATGAGATG-3′), AIV-H9-B3

(5′-AATGGTTTGAAGGCCCTAT-3′), AIV-H9-LF (5′-GTGTATTGGGCGTCTTGAATAGG-3′), and AIV-H9-LB (5′-ACGCAGACAGATCTGTACACA-3′).[36] RT-LAMP samples (20 μL) comprised 1× isothermal amplification buffer, AIV-H9-FIP (1.6 μM), AIV-H9-BIP (1.6 μM), AIV-H9-F3 (0.2 μM), AIV-H9-B3 (0.2 μM), AIV-H9-LF (0.8 μM), AIV-H9-LB (0.8 μM), amine-QDs (40 nM), AMV reverse transcriptase (0.025 units/μL), betaine (0.2 M), *Bst* 2.0 DNA polymerase (0.4 units/μL), dNTPs (1.4 mM; 0.35 mM each), and purified RNA extract (1 μL of different dilutions; 10^{-3}–10^{-6}). After incubation at 65 °C for 40 min, the samples were visualized under ultraviolet excitation (365 nm). Agarose gel electrophoresis analysis of the samples was also conducted (same protocol as that for lambda DNA). Two RT-qPCR primers and one TaqMan probe were utilized for amplifying and detecting avian influenza virus RNA (H9 subtype), including AIV-H9-F (5′-ATTTATTCGACTG(C/T)CGCC-3′), AIV-H9-R (5′-ATGTT GCA(C/T) CTGCAAGA-3′), and AIV-H9-P (5′-FAM-TGC(A/G)AT(A/G)GGGTTTGCGCC-BHQ1-3′).[37] For RT-qPCR assays, samples (20 μL) comprised 1× QuantiFast Pathogen Master Mix, 1× QuantiFast Pathogen RT Mix, 1× Internal Control Assay, 1× Internal Control RNA, AIV-H9-F (0.4 μM), AIV-H9-R (0.4 μM), AIV-H9-P (0.2 μM), and purified RNA extract (1 μL of different dilutions; 10^{-3}–10^{-6}). Temperature profile involved RT at 50 °C for 20 min, initial denaturation at 95°C for 5 min, followed by 45 thermal cycles of denaturation at 95 °C for 15 s and annealing/extension at 60 °C for 30 s. All RT-qPCR assays were performed in duplicate.

3. RESULTS AND DISCUSSION

3.1. Synthesis and Characterization of Amine-QDs. Oleic acid-capped CdSeS/ZnS QDs (diameter of 6 nm; emission peak at 540 nm, green color; dispersed in toluene) were used as the

starting material. By means of ligand/thiol exchange with cysteamine,[32] amine-functionalized QDs (amine-QDs) were prepared (dispersed in water and purified by centrifugal ultrafiltration). The prepared amine-QDs exhibited a characteristic absorption peak at 517 nm (Figure S1), identical to that of oleic acid-capped CdSeS/ZnS QDs (information provided by the manufacturer). The prepared amine-QDs had a zeta potential of +5.1 mV at pH 9 and gradually increased to +33.1 mV at pH 5 (Figure S2). This provides evidence for the successful amine functionalization of QDs (pK_a of amine in cysteamine: 10.75). Notably, in a LAMP reaction mixture (pH 8.8), amine-QDs would be positively charged.

3.2. Mechanistic Study of Dispersion and Precipitation Behavior of Amine-QDs under Simulated LAMP Conditions. The dispersion and precipitation behavior of amine-QDs was first studied with simulated LAMP solutions. The simulated negative LAMP solution contained 1× isothermal amplification buffer (comprising 2 mM $MgSO_4$; pH 8.8), while the simulated positive LAMP solution contained 1× isothermal amplification buffer and 1.4 mM $K_4P_2O_7$. For a positive LAMP sample (presence of target sequence), in addition to target sequence amplification, $P_2O_7^{4-}$ ions are produced, which complex with Mg^{2+} ions (present in nucleic acid amplification reactions as enzyme cofactor) to form insoluble $Mg_2P_2O_7$ crystals.[22,23] As shown in Figure 1a, the size of each individual $Mg_2P_2O_7$ crystal was ~0.5–0.8 μm. These crystals are likely spherical clusters of thin and plate-like structures.[38] When amine-QDs (60 nM) were present in the simulated negative LAMP solution, after incubation at 65 °C for 1 h, they remained well dispersed (Figure 1b; uniform green fluorescence upon 365 nm ultraviolet excitation). The dispersion was attributed to the electrostatic repulsion between positively charged amine-QDs. On the other hand, when amine-QDs were present in the simulated positive LAMP solution, they became precipitated (Figure 1c; green fluorescent precipitate; nonfluorescent supernatant). TEM along with EDS elemental

mapping analysis of the green fluorescent precipitate indicated the coexistence of amine-QDs and $Mg_2P_2O_7$ crystals (Figure 1d), suggesting the binding and coprecipitation between amine-QDs and $Mg_2P_2O_7$ crystals (note: $Mg_2P_2O_7$ crystals were mostly dispersed in the absence of amine-QDs; i.e., the simulated positive LAMP sample in Figure 1a). Electrostatic attraction and hydrogen bonding are very likely responsible for the binding. Zeta potentials of $Mg_2P_2O_7$ crystals, amine-QDs, and amine-QDs with $P_2O_7^{4-}$ at pH 8.8 (LAMP reaction condition) were measured (Figure S3). Notably, amine-QDs became negatively charged in the presence of $P_2O_7^{4-}$ (amine-QDs: +4.9 mV; amine-QDs with $P_2O_7^{4-}$: −22.4 mV), providing evidence for the strong binding between amine-QDs and $P_2O_7^{4-}$.

Confocal microscopy analysis was conducted to unravel whether amine-QDs were embedded in $Mg_2P_2O_7$ crystals or bound on the surface of $Mg_2P_2O_7$ crystals only. When the green fluorescent precipitate of the simulated positive LAMP sample (Figure 2a; identical to Figure 1c) was viewed under a confocal microscope, uniform green fluorescence was observed at all depths (Figure 2b; only one depth is shown), indicating that amine-QDs were embedded in $Mg_2P_2O_7$ crystals. As a comparison, amine-QDs only bound on the surface of $Mg_2P_2O_7$ crystals was examined, which was prepared by preforming $Mg_2P_2O_7$ crystals before adding amine-QDs. Figure 2a shows that, with preformed $Mg_2P_2O_7$ crystals, amine-QDs were also precipitated. As expected, when viewed under a confocal microscope, only the periphery of each individual $Mg_2P_2O_7$ crystal was lit up (Figure 2b). Taken together, these results confirmed that amine-QDs were embedded in (also bound on the surface of) $Mg_2P_2O_7$ crystals and thus led to their coprecipitation. Besides, it is important to note that amine-QDs remained dispersed in simulated negative LAMP solution containing deoxynucleoside triphosphates (dNTPs; precursors of $P_2O_7^{4-}$; Figure S4).

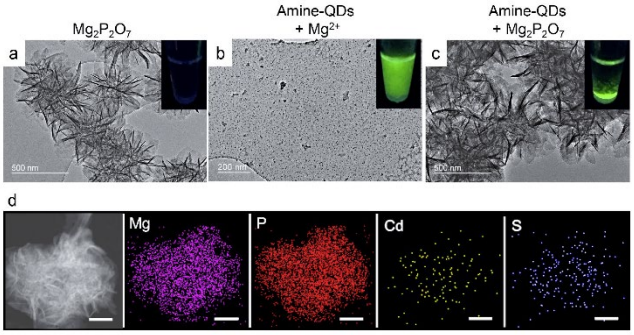

Figure 1. Dispersion and precipitation behavior of amine-QDs under simulated LAMP conditions. Fluorescence photographs (365 nm ultraviolet excitation) and transmission electron microscopy (TEM) images of (a) simulated positive LAMP sample (1× isothermal amplification buffer and 1.4 mM $K_4P_2O_7$); (b) simulated negative LAMP sample (1× isothermal amplification buffer) with 60 nM amine-QDs; and (c) simulated positive LAMP sample (1× isothermal amplification buffer and 1.4 mM $K_4P_2O_7$) with 60 nM amine-QDs. 1× isothermal amplification buffer contains 20 mM Tris-HCl, 10 mM $(NH_4)_2SO_4$, 50 mM KCl, 2 mM $MgSO_4$, and 0.1% Tween 20 (pH 8.8). The samples were incubated at 65 °C for 1 h. (d) Energy-dispersive X-ray spectroscopy elemental mapping images of the TEM sample in c; scale bars are 200 nm.

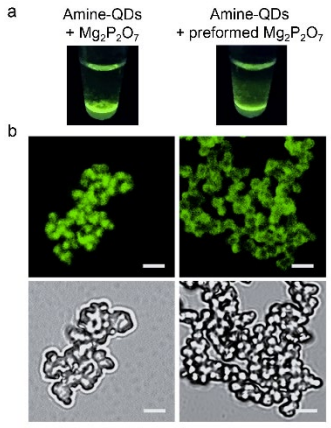

Figure 2. (a) Fluorescence photographs and (b) confocal microscopy images (top: fluorescence; bottom: bright field) of: (left column "Amine-QDs + $Mg_2P_2O_7$") simulated positive LAMP sample

(1× isothermal amplification buffer and 1.4 mM $K_4P_2O_7$) with 60 nM amine-QDs incubated at 65 °C for 1 h; (right column "Amine-QDs + preformed $Mg_2P_2O_7$") simulated positive LAMP sample incubated at 65 °C for 30 min, followed by the addition of amine-QDs and incubation at 65 °C for 1 h. Scale bars are 2 μm.

3.3. LAMP with Lambda DNA. Lambda DNA was chosen as the first model target sequence to prove the ability of amine-QDs to differentiate between negative (absence of target sequence) and positive (presence of target sequence) LAMP samples (note: one-step LAMP, i.e., amine-QDs being added to the reaction mixture before LAMP). After incubation at 65 °C for 1 h, amine-QDs remained dispersed in the negative LAMP sample (0 copies of lambda DNA; uniform green fluorescence upon 365 nm ultraviolet excitation; Figure 3c), but became precipitated in the positive LAMP sample (10^5 copies of lambda DNA; green fluorescent precipitate and weakly fluorescent supernatant; Figure 3d), consistent with the simulated results in Section 3.2 (Figures 1b and 1c). For the controls without amine-QDs, both the negative and positive LAMP samples showed no fluorescence under UV illumination (Figures 3a and 3b), but the positive LAMP sample showed turbidity under weak light condition (Figure S5). These samples were also analyzed by TEM (Figures 3a–d) and the results were again consistent with the simulated results (Figures 1a–c). Besides, these samples were further analyzed by agarose gel electrophoresis (Figure 3e). The characteristic ladder-like bands of the positive LAMP samples confirmed the successful amplification. Moreover, the intensities of the bands of the positive sample with amine-QDs were comparable to that of the positive LAMP sample without amine-QDs (lane 4 versus lane 2), indicating the excellent compatibility (i.e., negligible inhibition) of amine-QDs with LAMP. To investigate whether the LAMP amplicons could induce the precipitation of amine-QDs (the

mechanistic study in Section 3.2 with simulated LAMP samples did not consider LAMP amplicons), a positive LAMP sample without amine-QDs was prepared (LAMP amplicons and $Mg_2P_2O_7$ crystals were produced) and centrifuged, then the supernatant containing the LAMP amplicons (not containing $Mg_2P_2O_7$ crystals) was mixed with amine-QDs. After incubation at 65 °C for 1 h, amine-QDs remained dispersed (Figure S6), providing additional evidence that the precipitation of amine-QDs in the positive LAMP sample was primarily associated with $Mg_2P_2O_7$ crystals.

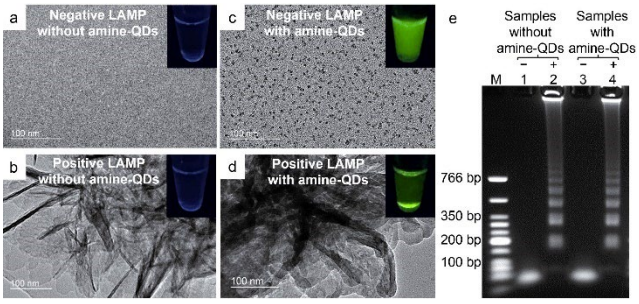

Figure 3. Amine-QD-based one-step LAMP assay for lambda DNA detection. Fluorescence photographs and TEM images of negative (0 copies) and positive (10^5 copies) samples with/without amine-QDs: (a) negative sample without amine-QDs; (b) positive sample without amine-QDs; (c) negative sample with amine-QDs; and (d) positive sample with amine-QDs. The concentrations of Mg^{2+} and amine-QDs (if any) were 2 mM and 40 nM, respectively. The samples were incubated at 65 °C for 1 h. (e) Agarose gel electrophoresis results of the samples in a–d. Lane M: DNA ladder; lane 1: sample in a; lane 2: sample in b; lane 3: sample in c; and lane 4: sample in d.

The specificity and sensitivity of this amine-QD-based one-step LAMP assay were evaluated. For specificity evaluation, lambda DNA and pBR322 DNA were employed as the specific and nonspecific templates, respectively. After incubation at 65 °C for 1 h, upon 365 nm ultraviolet excitation, the samples with no templates as well as with the nonspecific template (10^5 copies) appeared as uniform green fluorescent dispersion (Figure 4a). On the other hand, the samples with the specific template (10^5 copies), no matter alone or along with the nonspecific templates (10^5 copies), showed distinct green fluorescent precipitate (Figure 4a). The fluorescence readout results were validated by agarose gel electrophoresis analysis (Figure S7). The gel results were identical to those of the parallel samples without amine-QDs. For sensitivity evaluation, different copy numbers of lambda DNA (0–10^5) were tested. Two sets of experiments with different concentrations of Mg^{2+}, dNTPs, and primers (two of the six primers; forward inner primer "lambda-FIP" and backward inner primer "lambda-BIP) were performed. For the lower concentrations set (2 mM Mg^{2+}, 1.4 mM dNTPs, and 0.8 μM primers), it was found that amine-QDs in the samples with 10^2 copies or less of lambda DNA remained as dispersion while amine-QDs in the samples with 10^3 copies or more ended up as partial precipitation (Figure 4b). For the higher concentrations set (8 mM Mg^{2+}, 5.6 mM dNTPs, and 1.6 μM primers), it was found that down to 1 copy could be detected (83 zM; reaction volume of 20 μL; Figure 4c). Compared with the qPCR gold standard test (Figure S8; 10 copies or more could be detected but not 1 copy) and other reported QD-based isothermal nucleic acid amplification assays (Table S1), the single-copy detection capability of this amine-QD-based one-step LAMP assay demonstrated its superior assay sensitivity performance. Analogous to the specificity test, the fluorescence readout results of the sensitivity test were validated by agarose gel electrophoresis analysis (Figure S9). As expected, the fluorescence readout results and the gel results for both sets of experiments matched perfectly.

It should be pointed out that the lower sensitivity for the lower concentrations set was not caused by amine-QDs (the gel results were identical to those of the parallel samples without amine-QDs; Figure S9a).

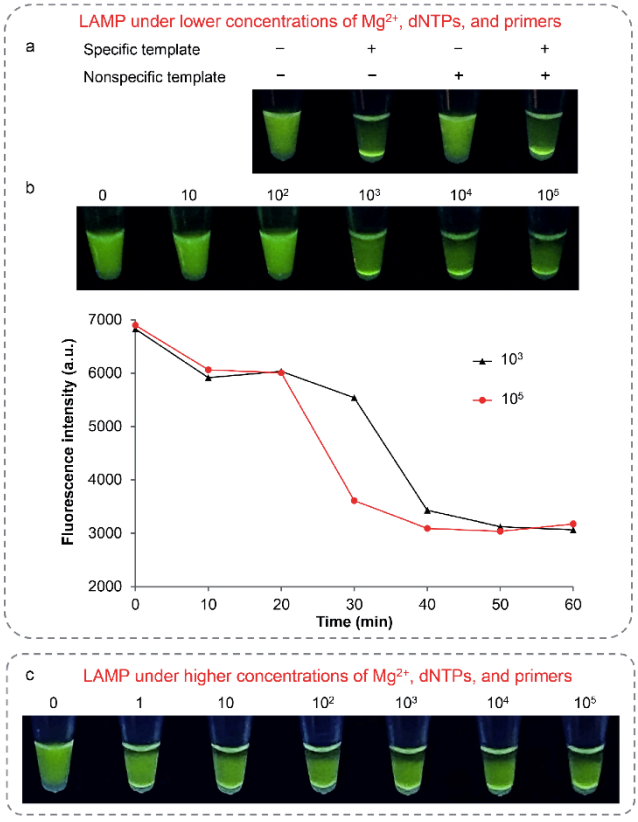

Figure 4. (a) Specificity and (b) sensitivity of the amine-QD-based one-step LAMP assay for lambda DNA detection under lower concentrations of Mg^{2+} (2 mM), dNTPs (1.4 mM total/0.35 mM each), and primers (lambda-FIP and lambda-BIP; 0.8 μM each). The concentration of amine-QDs was 40 nM. The samples were incubated at 65 °C for 1 h. (a) Fluorescence photograph showing the results of four samples with different template combinations of lambda DNA (specific template) and pBR322 DNA (nonspecific template): (from left to right) no template; lambda DNA only; pBR322 DNA only; and lambda DNA plus pBR322 DNA. The copy number of both

templates was 10^5. (b) (Top) Fluorescence photograph showing the results of samples with different copy numbers of lambda DNA (0–10^5) and (bottom) plots of fluorescence intensity versus LAMP reaction time for the samples with 10^3 or 10^5 copies of lambda DNA. (c) Sensitivity of the amine-QD-based one-step LAMP assay for lambda DNA detection under higher concentrations of Mg^{2+} (8 mM), dNTPs (5.6 mM total/1.4 mM each), and primers (lambda-FIP and lambda-BIP; 1.6 μM each). The samples were incubated at 65 °C for 40 min. Fluorescence photograph showing the results of samples with different copy numbers of lambda DNA (0–10^5; triplicate for each; only one set of the triplicate is shown).

The end-point readout above could only provide qualitative results. In fact, quantitative assay can be achieved by means of real-time monitoring of the precipitation process of amine-QDs during LAMP (e.g., fluorescence excitation light source passing through the supernatant). Attempt was made to measure the supernatant fluorescence of the samples with 10^3 or 10^5 copies in the previous sensitivity test (lower concentrations set). As shown in Figure 4b, a sharp decrease in the supernatant fluorescence intensity was observed from 30 min to 40 min for the sample with 10^3 copies and from 20 min to 30 min for the sample with 10^5 copies. A threshold fluorescence intensity can be defined to determine the threshold time for a positive sample of certain specific template copy number. As expected, the higher the copy number, the shorter the threshold time. For a threshold fluorescence intensity of 4,500 (Figure 4b), the threshold time for 10^5 copies is 26 min whereas the threshold time for 10^3 copies is 34 min. With a wider range of template copy numbers (e.g., 10^0, 10^1, 10^2, 10^3, 10^4, 10^5, and 10^6), a calibration curve can be obtained by plotting threshold time versus copy number (log scale). In fact, this is similar to plotting threshold cycle versus copy number (log scale) for qPCR/RT-qPCR.

3.4. RT-LAMP with SARS-CoV-2 RNA. Severe acute respiratory syndrome coronavirus 2 (SARS-CoV-2; the causative agent of coronavirus disease 2019, COVID-19) RNA was chosen to demonstrate the applicability of amine-QDs for one-step RT-LAMP assay. Figure 5 shows the sensitivity tests targeting the nucleocapsid (N) gene and the envelope (E) gene. After incubation at 65 °C for 40 min, for both the N and E genes, all the positive samples (1, 10, and 100 copies; partial precipitation of amine-QDs, obvious green fluorescent precipitate) were clearly distinguishable from the negative sample (0 copies; well dispersion of amine-QDs, uniform green fluorescence). The fluorescence readout results were confirmed by agarose gel electrophoresis analysis (Figure S10). The single-copy detection capability of this amine-QD-based one-step RT-LAMP compared favorably with RT-qPCR (for the E gene, 10 copies could be detected but not 1 copy, same as lambda DNA with qPCR; for the N gene, 100 copies could be detected but not 10 copies; Figure 5). For specificity test with this amine-QD-based one-step RT-LAMP (primers specific to SARS-CoV-2 RNA), 11 nonspecific templates were tested, including *Bordetella pertussis* DNA, *Haemophilus influenzae* DNA, influenza A H1 RNA, Middle East respiratory syndrome coronavirus RNA, *Mycobacterium tuberculosis* DNA, *Mycoplasma pneumoniae* DNA, parainfluenza 1 RNA, parainfluenza 4A RNA, rhinovirus RNA, SARS (2003) coronavirus RNA, and *Streptococcus pneumoniae* DNA. As shown in Figure S11, after incubation at 65 °C for 35 min, green fluorescent precipitates only occurred in the samples containing the specific template (SARS-CoV-2 RNA; alone or in the presence of all other 11 nonspecific templates), demonstrating the excellent specificity of this amine-QD-based one-step RT-LAMP assay platform.

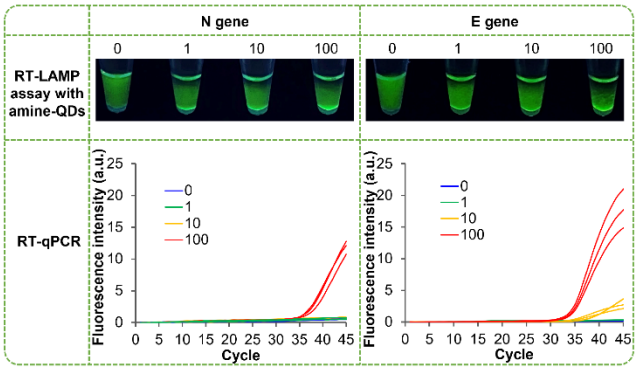

Figure 5. (Top) Sensitivity of the amine-QD-based one-step RT-LAMP assay for severe acute respiratory syndrome coronavirus 2 (SARS-CoV-2) RNA (nucleocapsid (N) gene and envelope (E) gene) detection. Fluorescence photographs showing the results of samples with different copy numbers of SARS-CoV-2 (0–100; triplicate for each; only one set of the triplicate is shown). (Bottom) Plots of fluorescence intensity versus cycle number for different copy numbers (0–100; triplicate for each) of SARS-CoV-2 in real-time reverse transcription–polymerase chain reaction (RT-qPCR).

3.5. RT-LAMP with Avian Influenza Virus RNA from Live Chicken Swab. To evaluate the performance of amine-QD-based one-step RT-LAMP assay for real application, oropharyngeal/cloacal swab samples from live chickens were tested for avian influenza virus (AIV) H9 subtype RNA. The samples were first processed to prepare purified RNA extracts. Then, different dilutions of the purified RNA extracts were prepared (10^3-fold dilution "10^{-3}" and 10-fold serial dilutions down to "10^{-6}"; Figure 6a). Figure 6b shows the fluorescence readout results of two swab samples after RT-LAMP (65 °C for 40 min). Amine-QDs of one sample were precipitated for 10^{-3}, 10^{-4}, and 10^{-5} dilutions but were dispersed for 10^{-6} dilution, indicative of a positive sample (presence of AIV H9 RNA) reaching single-copy level at 10^{-5} dilution. On the other hand, amine-QDs of another sample were dispersed for all the dilutions, indicative of a

negative sample (absence of AIV H9 RNA). The amplification results were verified by agarose gel electrophoresis analysis (Figure S12). RT-qPCR was also performed for further verification of the two swab samples. The results confirmed that one sample was positive and another sample was negative (Figure 6c), consistent with the amine-QD-based one-step RT-LAMP results. It should be noted that, with RT-qPCR, the positive sample was detectable down to 10^{-4} dilution only (versus 10^{-5} dilution with amine-QD-based one-step RT-LAMP). In fact, such 10-fold improvement in the assay sensitivity was also observed with lambda DNA and SARS-CoV-2 RNA.

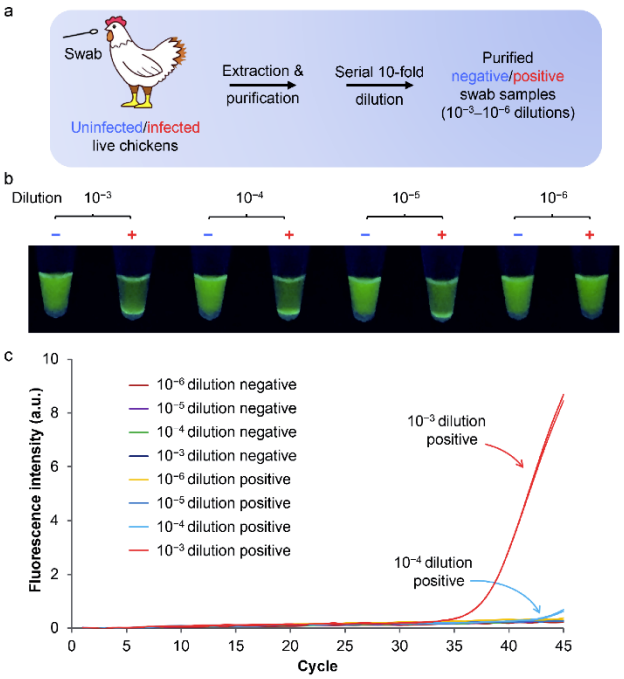

Figure 6. Avian influenza virus (H9 subtype) RNA detection from live chicken swab samples. (a) Schematic illustration of the sample preparation steps. (b) Fluorescence photograph showing the amine-QD-based one-step RT-LAMP results of serially diluted (10^{-3}–10^{-6}) H9 negative "–" and

positive "+" samples. (c) Plots of fluorescence intensity versus cycle number for different dilutions (10^{-3}–10^{-6}; duplicate for each) of H9 negative and positive samples in RT-qPCR.

4. CONCLUSIONS

We developed a new nucleic acid assay platform based on amine-QDs and LAMP/RT-LAMP, which is a first-of-its-kind one-step isothermal nucleic acid amplification coupled with quantum dot fluorescent reporter. The amine-functionalization, rendering QDs positively charged, enabled the differentiation between negative (absence of a target nucleic acid sequence) and positive (presence of a target nucleic acid sequence) samples. For the negative sample, amine-QDs were dispersed due to interparticle electrostatic repulsion. For the positive sample, amine-QDs were precipitated due to binding and coprecipitation between amine-QDs and $Mg_2P_2O_7$ crystals. With lambda DNA and SARS-CoV-2 as model targets, single-copy assay sensitivity (83 zM; reaction volume of 20 μL) was demonstrated. Besides, AIV H9 RNA from live chicken swab sample was successfully detected. With the simple constant temperature control and short assay time of LAMP/RT-LAMP as well as the excellent photostability of QDs, this amine-QD-based one-step LAMP/RT-LAMP assay has great potential as an alternative gold standard to qPCR/RT-qPCR assay, in particular for decentralized (point-of-care and on-site) nucleic acid testing. Toward this goal, it is essential to determine the analytical and clinical performance characteristics of this amine-QD-based one-step LAMP/RT-LAMP assay. LOD will be determined using serial dilutions of purified DNA/RNA controls (at least 20 replicates for 95% confidence). Clinical sensitivity, specificity, and accuracy will be determined using clinical samples (with reference to qPCR/RT-qPCR assay). In addition, for real-world applications, it is ideal to run the assay with a handheld/portable device for real-time monitoring of the amine-QDs precipitation.

ASSOCIATED CONTENT

Supporting Information

Visible absorption spectrum and pH-dependent zeta potentials of amine-QDs; zeta potential of amine-QDs with $P_2O_7^{4-}$; dispersion/precipitation behavior of amine-QDs in the presence of dNTPs or LAMP amplicons; turbidity of positive LAMP sample without amine-QDs; comparison of QD-based isothermal nucleic acid amplification assay platforms; agarose gel electrophoresis results of the amine-QD-based LAMP/RT-LAMP assays for lambda DNA, SARS-CoV-2 RNA, and avian influenza virus (H9 subtype) RNA; specificity of the amine-QD-based one-step RT-LAMP assay for SARS-CoV-2 RNA detection; and qPCR assay results for lambda DNA

AUTHOR INFORMATION

Corresponding Authors

E-mails: shea.ping.yip@polyu.edu.hk (Shea Ping Yip); ming-hung.lee@polyu.edu.hk (Thomas M. H. Lee)

Author Contributions

§S.W. and A.Q. contributed equally to this work. S.W. performed all the experiments and drafted the manuscript. A.Q. performed some initial experiments and drafted the manuscript. L.Y.C. assisted in the characterization of amine-QDs. E.W.T.F., M.Y.C., and C.J.B. provided the purified

chicken swab samples. G.K.H.S., C.-L.H., S.P.Y., and T.M.H.L. provided guidance on data analysis. S.P.Y. and T.M.H.L. revised the manuscript.

Notes

The authors declare no competing financial interest.

ACKNOWLEDGMENTS

This work is supported by the General Research Fund from the Research Grants Council of Hong Kong (project number: 15304417), Health and Medical Research Fund from the Food and Health Bureau of Hong Kong (project number: COVID190208), and Inter-Faculty Collaboration Scheme from The Hong Kong Polytechnic University (project number: P0038414).

REFERENCES

(1) Wilhelm, J.; Pingoud, A. Real-Time Polymerase Chain Reaction. *ChemBioChem* **2003**, *4*, 1120–1128.

(2) Zhao, Y.; Chen, F.; Li, Q.; Wang, L.; Fan, C. Isothermal Amplification of Nucleic Acids. *Chem. Rev.* **2015**, *115*, 12491–12545.

(3) Compton, J. Nucleic Acid Sequence-Based Amplification. *Nature* **1991**, *350*, 91–92.

(4) Walker, G. T.; Fraiser, M. S.; Schram, J. L.; Little, M. C.; Nadeau, J. G.; Malinowski, D. P. Strand Displacement Amplification—An Isothermal, in Vitro DNA Amplification Technique. *Nucleic Acids Res.* **1992**, *20*, 1691–1696.

(5) Fire, A.; Xu, S.-Q. Rolling Replication of Short DNA Circles. *Proc. Natl. Acad. Sci. U. S.* A. **1995**, *92*, 4641–4645.

(6) Notomi, T.; Okayama, H.; Masubuchi, H.; Yonekawa, T.; Watanabe, K.; Amino, N.; Hase, T. Loop-Mediated Isothermal Amplification of DNA. *Nucleic Acids Res.* **2000**, *28*, e63.

(7) Van Ness, J.; van Ness, L. K.; Galas, D. J. Isothermal Reactions for the Amplification of Oligonucleotides. *Proc. Natl. Acad. Sci. U. S. A.* **2003**, *100*, 4504–4509.

(8) Vincent, M.; Xu, Y.; Kong, H. Helicase-Dependent Isothermal DNA Amplification. *EMBO Rep.* **2004**, *5*, 795–800.

(9) Piepenburg, O.; Williams, C. H.; Stemple, D. L.; Armes, N. A. DNA Detection Using Recombination Proteins. *PLoS Biol.* **2006**, *4*, e204.

(10) Chen, H.-W.; Weissenberger, G.; Ching, W.-M. Development of Lyophilized Loop-Mediated Isothermal Amplification Reagents for the Detection of *Leptospira*. *Milit. Med.* **2016**, *181*, 227–231.

(11) Song, X.; Coulter, F. J.; Yang, M.; Smith, J. L.; Tafesse, F. G.; Messer, W. B.; Reif, J. H. A Lyophilized Colorimetric RT-LAMP Test Kit for Rapid, Low-Cost, At-Home Molecular Testing of SARS-CoV-2 and Other Pathogens. *Sci. Rep.* **2022**, *12*, 7043.

(12) Kaneko, H.; Kawana, T.; Fukushima, E.; Suzutani, T. Tolerance of Loop-Mediated Isothermal Amplification to a Culture Medium and Biological Substances. *J. Biochem. Biophys. Methods* **2007**, *70*, 499–501.

(13) Francois, P.; Tangomo, M.; Hibbs, J.; Bonetti, E.-J.; Boehme, C. C.; Notomi, T.; Perkins, M. D.; Schrenzel, J. Robustness of a Loop-mediated Isothermal Amplification Reaction for Diagnostic Applications. *FEMS Immunol. Med. Microbiol.* **2011**, *62*, 41–48.

(14) Lai, M. Y.; Suppiah, J.; Thayan, R.; Ismail, I.; Mustapa, N. I.; Tuan Soh, T. S.; Hassan, A. H.; Peariasamy, K. M.; Lee, Y. L.; Lau, Y. L. RNA Purification-Free Detection of SARS-CoV-2 Using Reverse Transcription Loop-Mediated Isothermal Amplification (RT-LAMP). *Trop. Med. Health* **2022**, *50*, 2.

(15) Dong, Y.; Zhao, Y.; Li, S.; Wan, Z.; Lu, R.; Yang, X.; Yu, G.; Reboud, J.; Cooper, J. M.; Tian, Z.; Zhang, C. Multiplex, Real-Time, Point-of-Care RT-LAMP for SARS-CoV-2 Detection Using the HFman Probe. *ACS Sens.* **2022**, *7*, 730–739.

(16) Ooi, K. H.; Liu, M. M.; Moo, J. R.; Nimsamer, P.; Payungpron, S.; Kaewsapsak, P.; Tan, M. H. A Sensitive and Specific Fluorescent RT-LAMP Assay for SARS-CoV-2 Detection in Clinical Samples. *ACS Synth. Biol.* **2022**, *11*, 448–463.

(17) Nagamine, K.; Hase, T.; Notomi, T. Accelerated Reaction by Loop-Mediated Isothermal Amplification Using Loop Primers. *Mol. Cell. Probes* **2002**, *16*, 223–229.

(18) Moehling, T. J.; Choi, G.; Dugan, L. C.; Salit, M.; Meagher, R. J. LAMP Diagnostics at the Point-of-Care: Emerging Trends and Perspectives for the Developer Community. *Expert Rev. Mol. Diagn.* **2021**, *21*, 43–61.

(19) Seyrig, G.; Stedtfeld, R. D.; Tourlousse, D. M.; Ahmad, F.; Towery, K.; Cupples, A. M.; Tiedje, J. M.; Hashsham, S. A. Selection of Fluorescent DNA Dyes for Real-Time LAMP with Portable and Simple Optics. *J. Microbiol. Methods* **2015**, *119*, 223–227.

(20) Quyen, T. L.; Ngo, T. A.; Bang, D. D.; Madsen, M.; Wolff, A. Classification of Multiple DNA Dyes Based on Inhibition Effects on Real-Time Loop-Mediated Isothermal Amplification (LAMP): Prospect for Point of Care Setting. *Front. Microbiol.* **2019**, *10*, 2234.

(21) Zhang, Y.; Tanner, N. A. Development of Multiplexed Reverse-Transcription Loop-Mediated Isothermal Amplification for Detection of SARS-CoV-2 and Influenza Viral RNA. *BioTechniques* **2021**, *70*, 167–174.

(22) Mori, Y.; Nagamine, K.; Tomita, N.; Notomi, T. Detection of Loop-Mediated Isothermal Amplification Reaction by Turbidity Derived from Magnesium Pyrophosphate Formation. *Biochem. Biophys. Res. Commun.* **2001**, *289*, 150–154.

(23) Mori, Y.; Kitao, M.; Tomita, N.; Notomi, T. Real-Time Turbidimetry of LAMP Reaction for Quantifying Template DNA. *J. Biochem. Biophys. Methods* **2004**, *59*, 145–157.

(24) Goto, M.; Honda, E.; Ogura, A.; Nomoto, A.; Hanaki, K.-I. Colorimetric Detection of Loop-Mediated Isothermal Amplification Reaction by Using Hydroxy Naphthol Blue. *BioTechniques* **2009**, *46*, 167–172.

(25) Tanner, N. A.; Zhang, Y.; Evans Jr., T. C. Visual Detection of Isothermal Nucleic Acid Amplification Using pH-Sensitive Dyes. *BioTechniques* **2015**, *58*, 59–68.

(26) Resch-Genger, U.; Grabolle, M.; Cavaliere-Jaricot, S.; Nitschke, R.; Nann, T. Quantum Dots versus Organic Dyes as Fluorescent Labels. *Nat. Methods* **2008**, *5*, 763–775.

(27) Bakalova, R.; Zhelev, Z.; Ohba. H.; Baba, Y. Quantum Dot-Conjugated Hybridization Probes for Preliminary Screening of siRNA Sequences. *J. Am. Chem. Soc.* **2005**, *127*, 11328–11335.

(28) Hu, J.; Liu, M.-H.; Zhang, C.-Y. Integration of Isothermal Amplification with Quantum Dot-Based Fluorescence Resonance Energy Transfer for Simultaneous Detection of Multiple microRNAs. *Chem. Sci.* **2018**, *9*, 4258–4267.

(29) Kuang, H.; Zhao, S.; Chen, W.; Ma, W.; Yong, Q.; Xu, L.; Wang, L.; Xu, C. Rapid DNA Detection by Interface PCR on Nanoparticles. *Biosens. Bioelectron.* **2011**, *26*, 2495–2499.

(30) He, S.; Huang, B.-H.; Tan, J.; Luo, Q.-Y.; Lin, Y.; Li, J.; Hu, Y.; Zhang, L.; Yan, S.; Zhang, Q.; Pang, D.-W.; Li, L. One-to-One Quantum Dot-Labeled Single Long DNA Probes. *Biomaterials* **2011**, *32*, 5471–5477.

(31) Cui, D.; Li, Q.; Huang, P.; Wang, K.; Kong, Y.; Zhang, H.; You, X.; He, R.; Song, H.; Wang, J.; Bao, C.; Asahi, T.; Gao, F.; Osaka, T. Real Time PCR Based on Fluorescent Quenching of Mercaptoacetic Acid-Modified CdTe Quantum Dots for Ultrasensitive Specific Detection of Nucleic Acids. *Nano Biomed. Eng.* **2010**, *2*, 45–55.

(32) Lee, C.-M.; Jang, D.; Cheong, S.-J.; Kim, E.-M.; Jeong, M.-H.; Kim, S.-H.; Kim, D. W.; Lim, S. T.; Sohn, M.-H.; Jeong, H.-J. Surface Engineering of Quantum Dots for in Vivo Imaging. *Nanotechnology* **2010**, *21*, 285102.

(33) Tambong, J. T.; Mwange, K. N.; Bergeron, M.; Ding, T.; Mandy, F.; Reid, L. M.; Zhu, X. Rapid Detection and Identification of the Bacterium *Pantoea stewartii* in Maize by TaqMan® Real-Time PCR Assay Targeting the *cpsD* Gene. *J. Appl. Microbiol.* **2008**, *104*, 1525–1537.

(34) Zhang, Y.; Ren, G.; Buss, J.; Barry, A. J.; Patton, G. C.; Tanner, N. A. Enhancing Colorimetric Loop-Mediated Isothermal Amplification Speed and Sensitivity with Guanidine Chloride. *BioTechniques* **2020**, *69*, 179–186.

(35) Corman, V. M.; Landt, O.; Kaiser, M.; Molenkamp, R.; Meijer, A.; Chu, D. K. W.; Bleicker, T.; Brunink, S.; Schneider, J.; Schmidt, M. L.; Mulders, D. G. J. C.; Haagmans, B. L.; van der Veer, B.; van den Brink, S.; Wijsman, L.; Goderski, G.; Romette, J.-L.; Ellis, J.; Zambon, M.; Peiris, M.; Goossens, H.; Reusken, C.; Koopmans, M. P. G.; Drosten, C. Detection of 2019 Novel Coronavirus (2019-nCoV) by Real-Time RT-PCR. *Euro Surveill.* **2020**, *25*, 2000045.

(36) Zou, M.; Xue, Q. H9 Subtype Avian Influenza Virus Loop-Mediated Isothermal Amplification Micro Total Analysis Method. *Chinese Patent* **2012**, CN102634607A. (https://patents.google.com/patent/CN102634607A/en)

(37) Das, A.; Suarez, D. L. Development and Bench Validation of Real-Time Reverse Transcription Polymerase Chain Reaction Protocols for Rapid Detection of the Subtypes H6, H9, and H11 of Avian Influenza Viruses in Experimental Samples. *J. Vet. Diagn. Invest.* **2007**, *19*, 625–634.

(38) Van Leeuwen, Y. M.; Velikov, K. P.; Kegel, W. K. Morphology of Colloidal Metal Pyrophosphate Salts. *RSC Adv.* **2012**, *2*, 2534–2540.

TABLE OF CONTENTS GRAPHIC

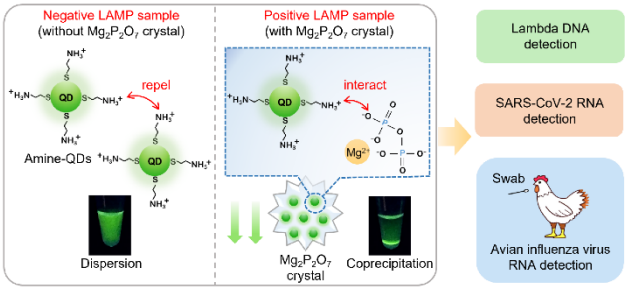

Supporting Information

Amine-Functionalized Quantum Dots as Universal Fluorescent Nanoprobe for One-Step Loop-Mediated Isothermal Amplification Assay with Single-Copy Sensitivity

Shiyao Wang,[a,§] Ailin Qin,[a,§] Li Yin Chau,[a] Eunice W. T. Fok,[b] Mei Yue Choy,[b] Christopher J. Brackman,[b] Gilman K. H. Siu,[c] Chien-Ling Huang,[c] Shea Ping Yip,[c,] and Thomas M. H. Lee[a,]**

[a]Department of Biomedical Engineering, The Hong Kong Polytechnic University, Hung Hom, Kowloon, Hong Kong 000000, China

[b]Agriculture, Fisheries and Conservation Department, Government of the Hong Kong Special Administrative Region, Hong Kong 000000, China

[c]Department of Health Technology and Informatics, The Hong Kong Polytechnic University, Hung Hom, Kowloon, Hong Kong 000000, China

[§]Shiyao Wang and Ailin Qin contributed equally to this work

*Corresponding authors. E-mails: shea.ping.yip@polyu.edu.hk (Shea Ping Yip); ming-hung.lee@polyu.edu.hk (Thomas M. H. Lee)

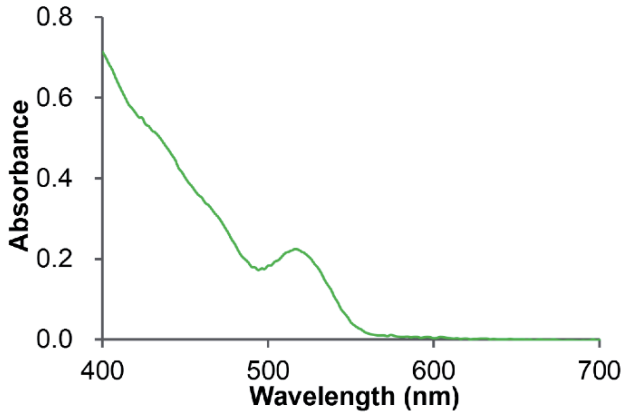

Figure S1. Visible absorption spectrum of amine-QDs.

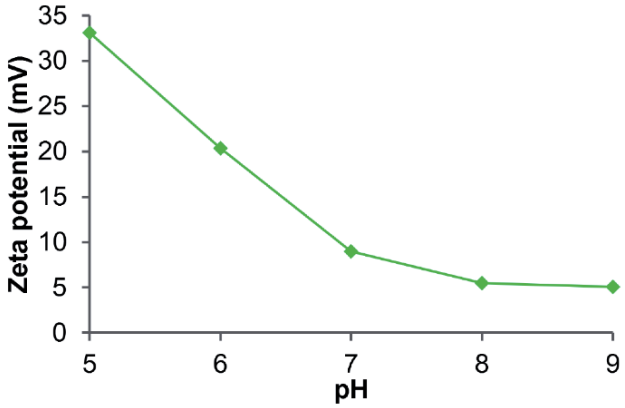

Figure S2. Plot of zeta potential versus pH of amine-QDs.

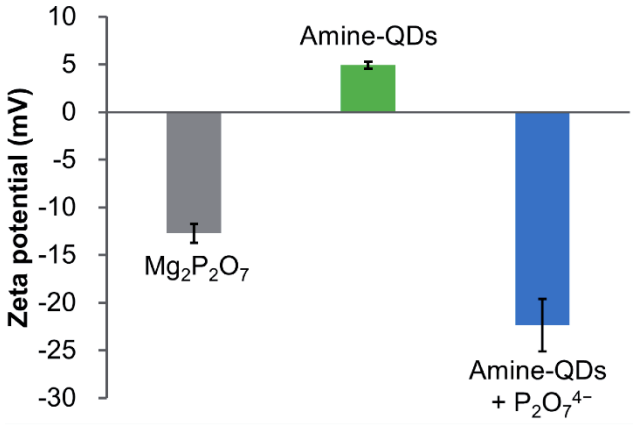

Figure S3. Zeta potentials of $Mg_2P_2O_7$ crystals, amine-QDs, and amine-QDs with $P_2O_7^{4-}$ at pH 8.8 (20 mM Tris-HCl). Error bars are calculated from three samples.

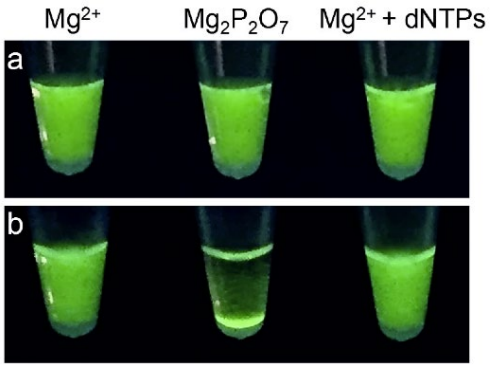

Figure S4. Fluorescence photographs (365 nm ultraviolet excitation) showing the dispersion and precipitation behavior of amine-QDs in: (left column "Mg^{2+}") 1× isothermal amplification buffer (20 mM Tris-HCl, 10 mM $(NH_4)_2SO_4$, 50 mM KCl, 2 mM $MgSO_4$, and 0.1% Tween 20; pH 8.8); (middle column "$Mg_2P_2O_7$") 1× isothermal amplification buffer with 1.4 mM $K_4P_2O_7$; and (right column "Mg^{2+} + dNTPs") 1× isothermal amplification buffer with 1.4 mM deoxynucleoside triphosphates (dNTPs; 0.35 mM each) (a) before and (b) after incubation at 65 °C for 1 h. The concentration of amine-QDs was 60 nM.

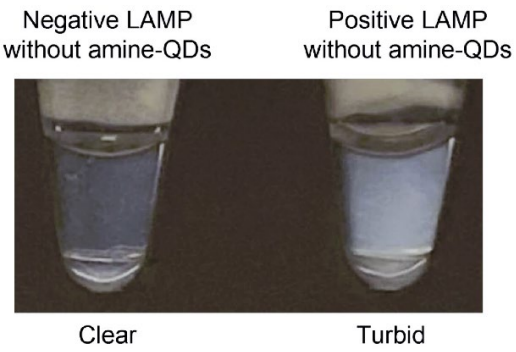

Figure S5. Photograph showing the negative and positive LAMP samples without amine-QDs after incubation at 65 ºC for 1 h (Figures 3a and 3b). Negative sample: 0 copies of lambda DNA; positive sample: 10^5 copies of lambda DNA. The photo was taken under weak light condition to show the turbidity difference.

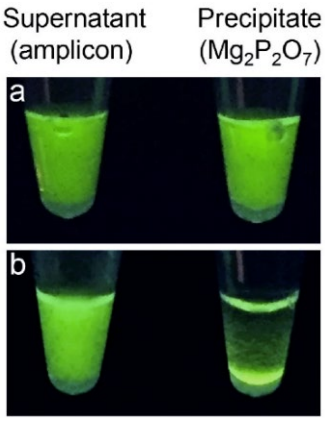

Figure S6. Fluorescence photographs showing the dispersion and precipitation behavior of amine-QDs (a) before and (b) after incubation at 65 °C for 1 h when added to the supernatant (amplicon) and precipitate ($Mg_2P_2O_7$ crystals) of the centrifuged positive LAMP sample.

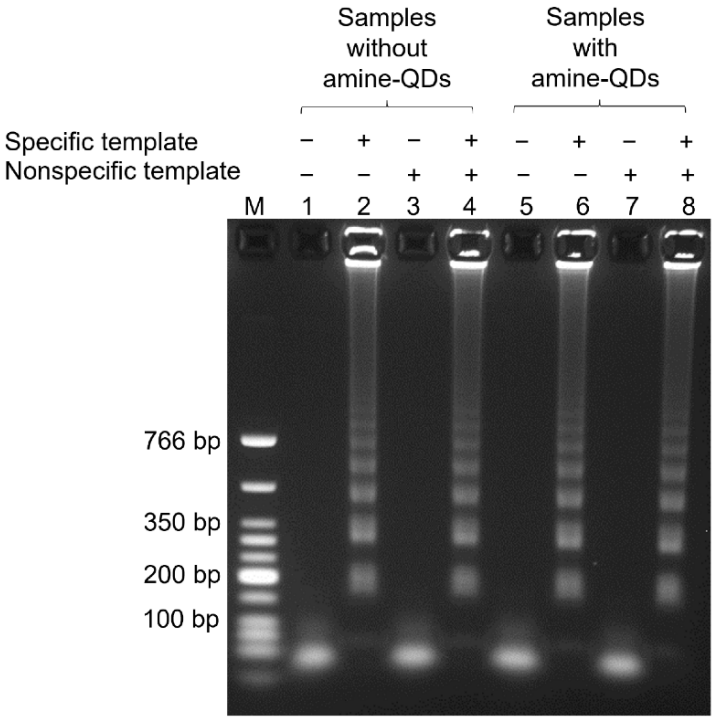

Figure S7. Agarose gel electrophoresis results of the specificity test of the amine-QD-based one-step LAMP assay for lambda DNA detection under lower concentrations of Mg^{2+}, dNTPs, and primers in Figure 4a. Different template combinations of lambda DNA (specific template) and pBR322 DNA (nonspecific template) were included. Lane M: DNA ladder; lanes 1–4: samples without amine-QDs; lanes 5–8: samples with amine-QDs; lanes 1 and 5: no template; lanes 2 and 6: lambda DNA only (10^5 copies); lanes 3 and 7: pBR322 DNA only (10^5 copies); and lanes 4 and 8: lambda DNA plus pBR322 DNA (10^5 copies each).

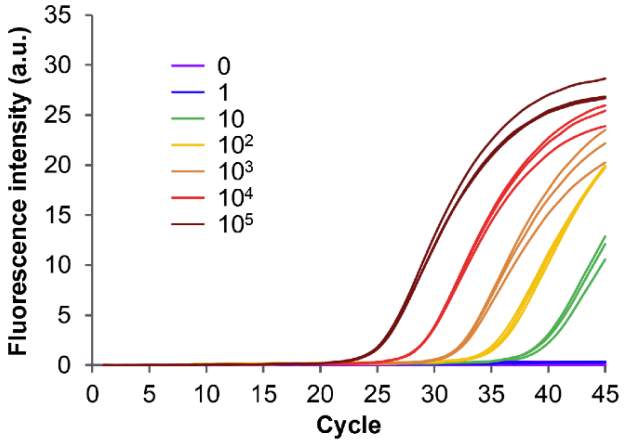

Figure S8. Plots of fluorescence intensity versus cycle number for different copy numbers (0–10^5; triplicate for each) of lambda DNA in real-time polymerase chain reaction (qPCR) assays.

Quantum dot probes	Isothermal nucleic acid amplification	Closed/open-tube detection format	Detection time (including amplification)	Limit of detection (LOD)	Reference
Oligo-QDs	NASBA	Open-tube	> 7 h	40 nM	27
Streptavidin-QDs	RCA	Open-tube	> 2.5 h	16 aM	28
Amine-QDs	LAMP	Closed-tube	< 40 min	83 zM	This work

Table S1. Comparisons of three QD-based isothermal nucleic acid amplification assay platforms.

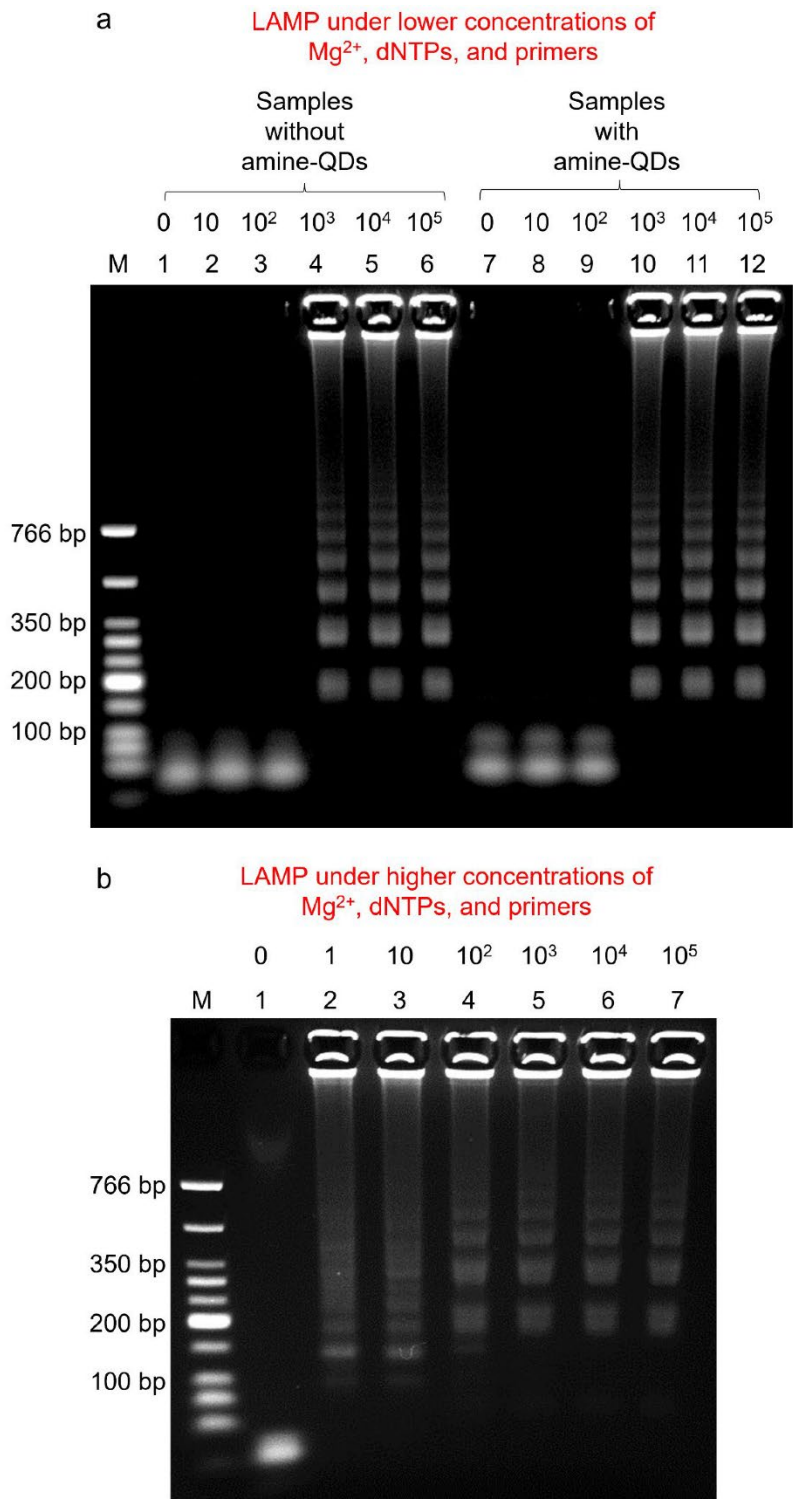

Figure S9. Agarose gel electrophoresis results of the sensitivity test of the amine-QD-based one-step LAMP assay for lambda DNA detection. Different copy numbers of lambda DNA (0–10^5) were included. (a) Lower concentrations of Mg^{2+}, dNTPs, and primers were used (corresponding

samples in Figure 4b). Lane M: DNA ladder; lanes 1–6: samples without amine-QDs; lanes 7–12: samples with amine-QDs; lanes 1–6 as well as lanes 7–12: 0, 10, 10^2, 10^3, 10^4, and 10^5 copies of lambda DNA. (b) Higher concentrations of Mg^{2+}, dNTPs, and primers were used (corresponding samples in Figure 4c). Lane M: DNA ladder; lanes 1–7: 0, 1, 10, 10^2, 10^3, 10^4, and 10^5 copies of lambda DNA.

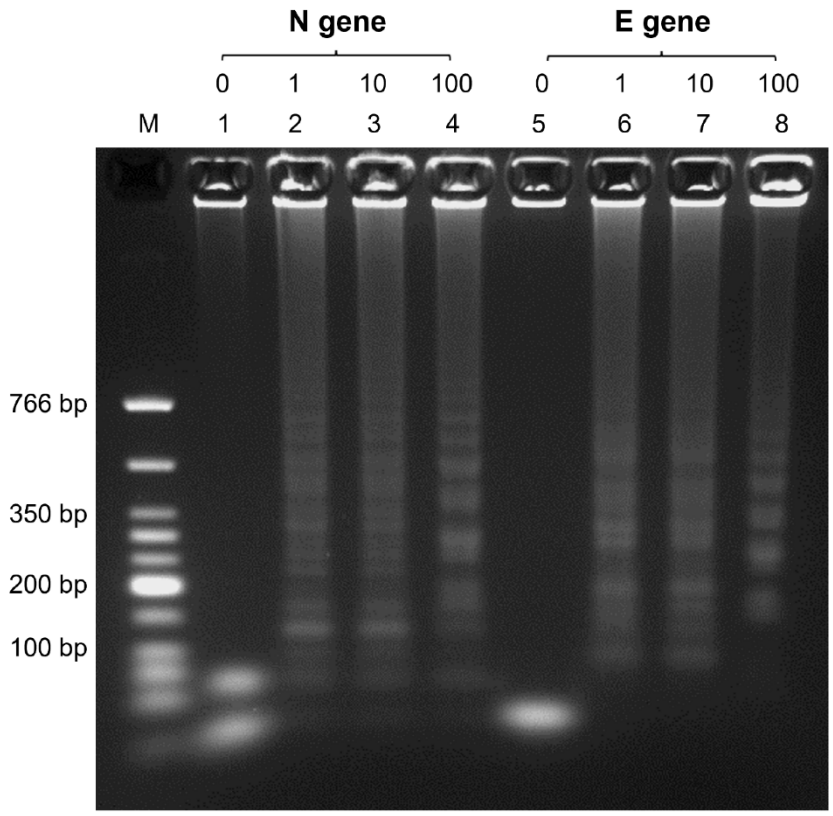

Figure S10. Agarose gel electrophoresis results of the sensitivity test of the amine-QD-based one-step RT-LAMP assay for SARS-CoV-2 RNA (N gene and E gene) detection in Figure 5. Lane M: DNA ladder; lanes 1–4: N gene; lanes 5–8: E gene; lanes 1 and 5: 0 copies of SARS-CoV-2 RNA; lanes 2 and 6: 1 copy of SARS-CoV-2 RNA; lanes 3 and 7: 10 copies of SARS-CoV-2 RNA; and lanes 4 and 8: 100 copies of SARS-CoV-2 RNA.

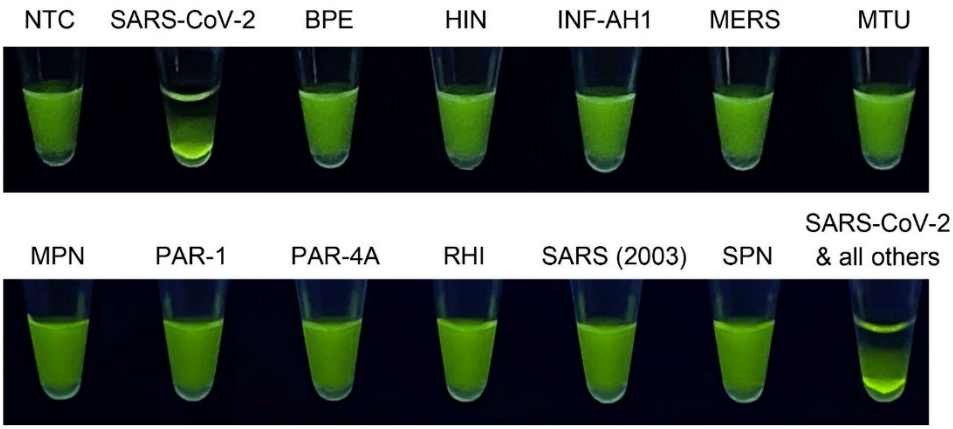

Figure S11. Specificity of the amine-QD-based one-step RT-LAMP assay for SARS-CoV-2 RNA (E gene) detection. Fluorescence photographs showing the results of samples with different templates (note: only SARS-CoV-2 was the specific template). NTC: no template control; BPE: *Bordetella pertussis* DNA; HIN: *Haemophilus influenzae* DNA; INF-AH1: influenza A H1 RNA; MERS: Middle East respiratory syndrome coronavirus RNA; MTU: *Mycobacterium tuberculosis* DNA; MPN: *Mycoplasma pneumoniae* DNA; PAR-1: parainfluenza 1 RNA; PAR-4A: parainfluenza 4A RNA; RHI: rhinovirus RNA; SARS (2003): SARS (2003) coronavirus RNA; SPN: *Streptococcus pneumoniae* DNA; and SARS-CoV-2 & all others: SARS-CoV-2 plus 11 nonspecific templates. The copy numbers of SARS-CoV-2 RNA and the nonspecific templates were 10^2 and 10^3, respectively. The samples were incubated at 65 °C for 35 min.

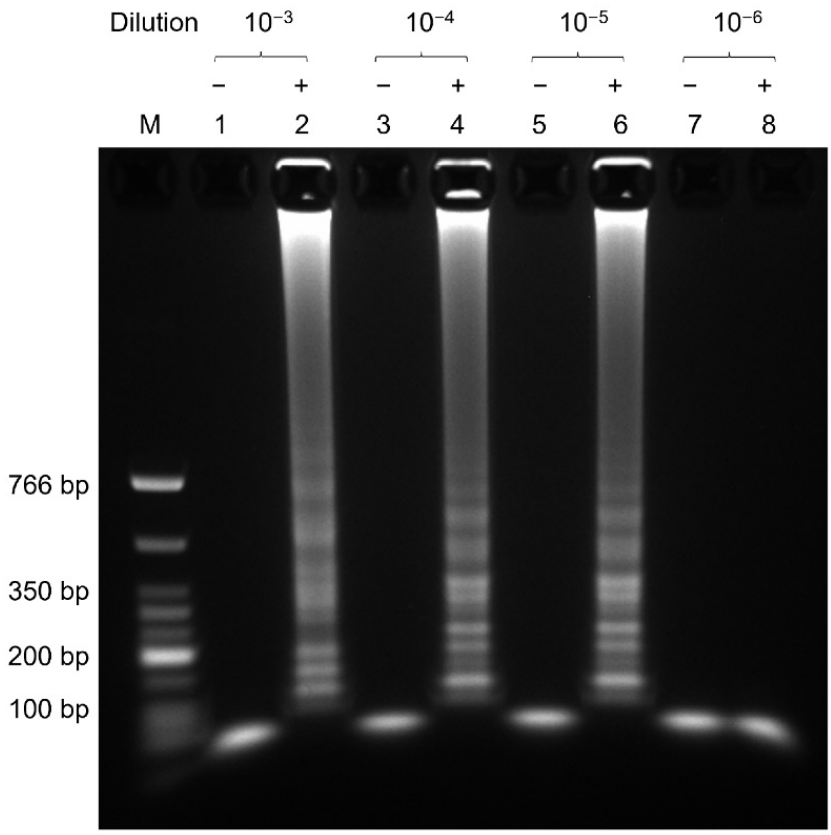

Figure S12. Agarose gel electrophoresis results of the amine-QD-based one-step RT-LAMP assay for serially diluted (10^{-3}–10^{-6}) H9 negative and positive samples in Figure 6b. Lane M: DNA ladder; lanes 1, 3, 5, and 7: negative; lanes 2, 4, 6, and 8: positive; lanes 1 and 2: 10^{-3} dilution; lanes 3 and 4: 10^{-4} dilution; lanes 5 and 6: 10^{-5} dilution; and lanes 7 and 8: 10^{-6} dilution.